A new cell for the collection of combined EXAFS/XRD data in situ during solid/liquid catalytic reactions

Ian J. Shannon [a], Thomas Maschmeyer [a], Gopinathan Sankar [a], John Meurig Thomas [a,*], Richard D. Oldroyd [a], Mike Sheehy [a], David Madill [a], Andrew M. Waller [b] and Rodney P. Townsend [b]

[a] *Davy Faraday Research Laboratory, The Royal Institution of Great Britain, 21 Albemarle Street, London W1X 4BS, UK*

[b] *Unilever Research, Port Sunlight Laboratory, Quarry Road East, Bebington, Wirral L63 3JW, UK*

Received 8 November 1996; accepted 10 December 1996

A new experimental reaction cell which enables the recording of combined EXAFS/XRD data over a wide range of temperatures of a solid that catalyses liquid reactions in the liquid state has been designed and constructed. The cell is particularly suitable for the in situ study of both short-range and long-range structural changes during solid/liquid heterogeneous catalytic reactions. It is also suitable for the study of intercalation phenomena and may be readily adapted for certain types of electrochemical investigations. The use of this cell is exemplified by the oxidation of cyclohexene over a Zn(II)Al(III)-hydrotalcite containing intercalated cobalt phthalocyaninetetrasulphonate anions.

Keywords: combined EXAFS/XRD, in situ studies, solid catalysts, hydrotalcites

1. Introduction

Advances in our understanding of the general phenomenology and specific attributes of heterogeneous catalysts are dependent on gaining more detailed determinations of structural changes that catalysts undergo during the actual processes of catalysis. Starting in 1988, two of us (JMT and RPT) in association with G.N. Greaves and C.R.A. Catlow [1,2], extended earlier work [3] in which X-ray diffraction (XRD) alone was tracked over a range of temperatures under in situ conditions, so as to determine the time-dependence of the redistribution of nickel ions within a zeolitic solid. Later, Maddox et al. [4] devised an in situ XRD method that showed how Ni^{2+} ions migrated from the so-called SI sites into the SII sites of the supercages of a Ni^{2+}-exchanged zeolite Y solid as it catalysed the cyclotrimerisation of acetylene to benzene; and Pickering et al. [5] improved that method further for XRD studies of the catalytic performance of $YBa_2Cu_3O_{6+x}$ in the oxidative dimerisation of methane [6].

But XRD alone, although valuable as a tool for monitoring the changes in crystallographic phase and, under optimal conditions [4,6], in the precise position of active sites, is not as powerful a structural tool as the combination of XRD and X-ray absorption (XRA) spectroscopy. In 1991, a collaboration between one of us and G.N. Greaves at the Daresbury Synchrotron Laboratory showed [7] how powerful the combined techniques of XRD/XRA – to be precise XRD and extended X-ray absorption fine structure (EXAFS) spectroscopy – are in elucidating the detailed solid state and surface structural changes exhibited by a precursor phase (the synthetic mineral aurichalcite) as it is converted in situ into an active Cu/ZnO catalyst for the reverse water–gas shift reaction. Others [8,9] have also described the advantages of the combined XRD/EXAFS approach for gas–solid heterogeneous catalytic reactions, and the various ways in which this approach may be conducted have been reviewed [10,11].

The use of a hydrothermal cell [12,13] to study kinetics of crystallisation [14] and intercalation [15] using energy dispersive X-ray diffraction has been demonstrated, while we ourselves have previously reported a capillary reactor cell to monitor the crystallisation of CoALPO-5 from a gel via combined EXAFS/XRD [16]. In situ catalytic studies using combined EXAFS/XRD have previously focused on solid/gas systems; for this purpose, capillary furnaces have been designed [9,17,18] through which it is possible continually to flow gaseous mixtures of known composition over the catalyst packed inside a quartz capillary. Homogeneous and heterogeneous catalysis in the liquid and solid/liquid states have been widely studied by EXAFS [19–21], but to our knowledge no one has previously extended these studies to utilise the combined EXAFS/XRD technique under in situ conditions.

2. Design of cell

The cell was designed of such dimensions as to fit within the configurational limits of Station 9.3 at Daresbury (fig. 1). The cell can also be used, with minor

* To whom correspondence should be addressed.

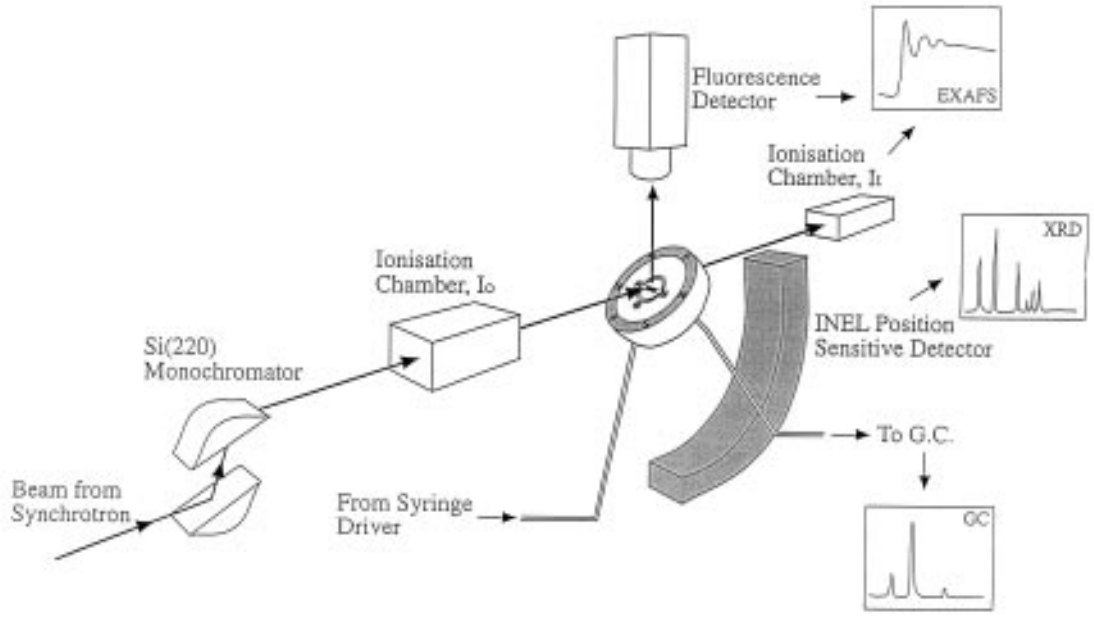

Fig. 1. Diagram showing the set up of the new solid/liquid experimental reactor cell for the parallel recording of EXAFS and XRD data on station 9.3 at the SRS facility at Daresbury. All paths for incoming and exiting beams are free from obstruction by the cell assembly.

modifications, to record EXAFS data on both Stations 8.1 and 9.2 of the Daresbury Laboratory under in situ catalytic conditions [22].

The cell (fig. 2) consists of a central stainless-steel body of diameter 57 mm, external depth 19 mm, and machined to a thickness of 1 mm across the face. All extraneous metal was machined out to ensure that there was no interference with the incoming or exiting beam or with the diffracted X-rays. A 20 mm $\times$ 1/2 mm deep recess was cut into the front face of the body, to accommodate a self-supporting wafer (20 mm diameter) of the catalyst under study, while a slot (2 $\times$ 10 mm) was cut through the centre to allow the recording of both transmission EXAFS and energy dispersive X-ray diffraction data. The catalyst was sandwiched between two Kapton^{TM} windows (thickness = 50 μm), held in place by means of brass clamping ring assemblies on either side of the sample area, generating a compression seal. Liquid reactants were passed through the sample area via syringe needles connected to two hollowed out screws, screwed into the main body of the cell, which pass through the back Kapton^{TM} window. A silicon rubber washer prevented leakage of the liquid reactants through these screw holes. A syringe driver (Harvard Apparatus) was used continuously to flow the reactants through the cell at atmospheric pressure, and the reac-

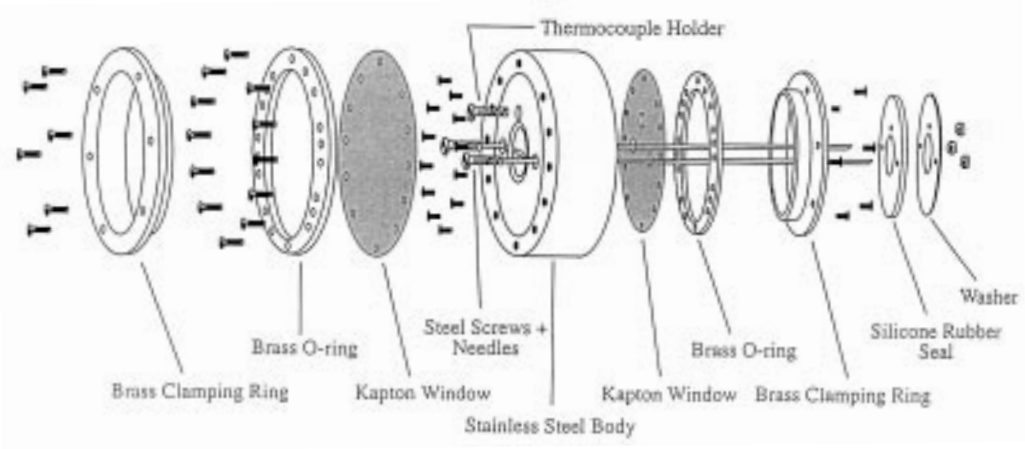

Fig. 2. Labelled diagram showing the construction of the solid/liquid experimental reactor cell. Leakproof seals around the sample area are generated through compression by the brass O-ring and clamping assembly.

tion products collected for analysis by GC and GC/MS. A third screw was partially hollowed to accommodate a thermocouple, to monitor the reaction temperature. By creating the cell in this way (i.e. all seals are generated by compression) we can use all solvents which are compatible with stainless steel, brass and Kapton™ as carriers for our reactants, which encompasses most of those commonly used. Solvents that are not suitable for use with this cell include alkalis and concentrated acids, which attack the Kapton™ windows and the stainless-steel body respectively.

Heating of the cell was achieved by one of two methods – either using a band heater clamped around the external diameter of the cell, or employing a jet of hot air directed onto the sample area through a nozzle [23]. The maximum temperature attainable is dictated by the boiling point of the solvent used in the reaction; the generation of gas bubbles in the liquid causes discontinuities in the EXAFS data. The Kapton™ windows are capable of withstanding temperatures up to ca. 250°C. While the band heater generates a small temperature gradient across the sample (< 10°C) due to heating from the outer diameter of the cell, the hot-air flow system allows for temperatures much closer to the boiling point of the solvent to be attained.

The quality of the transmission EXAFS data obtained is generally poor due to the high absorbance of the liquid in the cell, and is also affected by "pinhole" effects due to any air bubbles formed. The intensity of the XRD data is also reduced, due to attenuation by the liquid, but the fluorescence data are comparable to that obtained previously from other in situ experiments [16,18], with good quality data – covering the entire pre-edge, near-edge and EXAFS regions – being obtained in ca. 5 min.

3. Experimental and results

As an illustrative example of the type of data that may be obtained from using the new in situ solid/liquid catalysis cell, we studied the oxidation of cyclohexene over Zn(II)Al(III)-hydrotalcite containing the cobalt phthalocyaninetetrasulphonate anion. The tetrasodium salt of cobalt phthalocyaninetetrasulphonate [$Na_4CoPcTS$] was prepared by literature methods [24].

Zn(II)Al(III)-hydrotalcite containing the cobalt phthalocyaninetetrasulphonate anion ($CoPcTS^{4-}$) was prepared by coprecipitation, at constant pH, of a solution of zinc and aluminium nitrates (Zn(II) : Al(III) ratio of 3 : 1) with a solution of $Na_4CoPcTS$/NaOH. The gel ($0.75Zn(NO_3)_2 : 0.25Al(NO_3)_3 : 0.125Na_4CoPcTS : 2.00NaOH : 222H_2O$) was aged, under autogeneous pressure conditions, at 90°C for 18 h, and then filtered and washed with distilled water until the pH was 7, and the filtrate was clear of any non-intercalated cobalt phthalocyaninetetrasulphonate anion.

X-ray powder diffraction data were measured on a Siemens D500 powder diffractometer, using monochromated Cu K_α radiation ($\lambda = 1.5418$ Å). The X-ray powder diffraction data (fig. 3) for Zn(II)Al(III)-hydrotalcite/$CoPcTS^{4-}$ shows a pattern characteristic of a hydrotalcite-type compound. The interlamellar *d*-spacing is calculated from the pattern to be ca. 23.0 Å in close agreement with that previously reported [25].

Combined QuEXAFS/XRD data were recorded [26] at the Daresbury, SRS facility on station 9.3. The station was equipped with a double-crystal Si(220) monochromator, ion chambers for measuring incident (I_0) and transmitted (I_t) beam intensities, and a thirteen-element fluorescence detector (Canberra). In the present study,

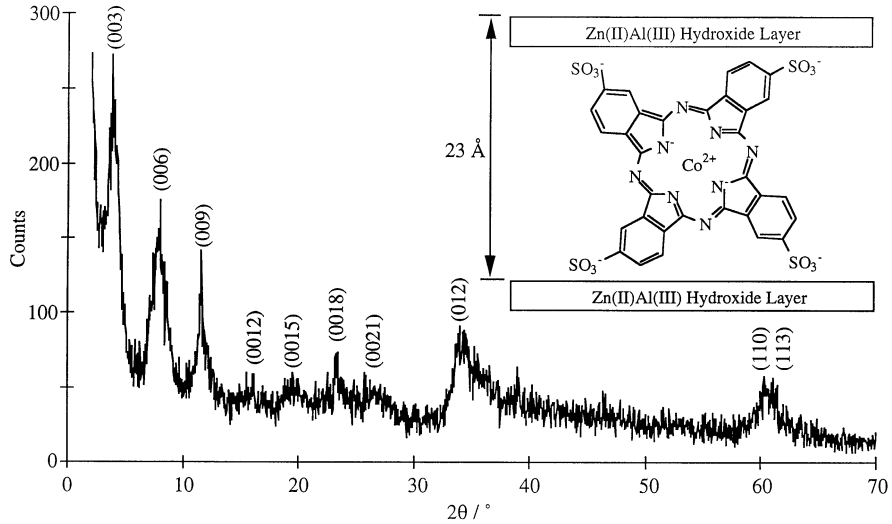

Fig. 3. Powder X-ray diffraction pattern, recorded on a laboratory X-ray diffractometer (Siemens D500), using Cu K_α radiation ($\lambda = 1.5406$ Å) for Zn(II)Al(III)-hydrotalcite containing cobalt phthalocyaninetetrasulphonate anions. The calculated *d*-spacing is ca. 23 Å, consistent with the sulphonated phthalocyanine ring of the intercalated anion being accommodated perpendicular to the metal hydroxide layers, as shown.

the fluorescence mode for XAS data collection was used. XRD measurements were recorded using a position sensitive INEL detector (PSD) at $\lambda = 1.4062$ Å. Although the INEL detector is suitable for collecting data up to 120°, the projections in the in situ cell limit the range to ca. 50° (note, however, by appropriate choice of the wavelength it is possible to record reflections occurring in both low or high 2θ regions). A typical beam size of 0.5 mm × 8 mm was obtained by employing an external slit. Spectra were recorded using sequential measurement of XRD and XAS during catalysis – turnaround time for the collection of each set of combined XAS/XRD data was 10 min (ca. 180 s for XRD, 380 s XAS, and 40 s deadtime). A self-supporting wafer of 100 mg Zn(II)Al(III)-hydrotalcite/$CoPcTS^{4-}$ was mounted in the cell, and reaction mixture composed of 0.5 M cyclohexene, 25 ml $CHCl_3$ and 0.70 g PhIO oxidant pumped through the reactor at a rate of 0.1 ml/min, while the sample environment was heated to ca. 30°C. In-house catalyst testing was carried out using 0.05 M cyclohexene, 2.5 ml $CHCl_3$ and 0.07 g PhIO with 1 ml of mesitylene added as internal standard. Typically 40 mg of catalyst were used and the reaction flask stirred at 30°C for 1 h before products were collected. GC analysis of the products collected showed selectivities of ca. 53% 2-cyclohexen-1-ol, 44% 2-cyclohexen-1-one, and 3% cyclohexeneoxide, with a low turnover frequency of 20 mol/(mol-catalyst h). The selectivity was found to be the same for the product collected from the in situ cell.

The suite of programs used to analyse the EXAFS data was that provided at Daresbury; the data were processed using the program EXCALIB, and background subtraction was carried out using EXBROOK. All fitting of the EXAFS oscillations was carried out using EXCURV92 [27]. Fitting of the EXAFS data for the catalyst prior to reaction (fig. 4), suggests that the local environment around the Co centre is distorted from the expected shell of 4 N neighbours to give two shells of 2 N neighbours at 1.94 and 2.14 Å.

In figs. 5a and 5b, XANES from the fluorescence EXAFS data and low-angle energy dispersive XRD data for the oxidation of cyclohexene over Zn(II)Al(III)-hydrotalcite containing cobalt phthalocyaninetetrasulphonate anions in the interlamellar region, recorded at 30°C using the new cell, are shown respectively. The simultaneous recording of EXAFS and XRD permits the monitoring of both changes in the EXAFS spectra and those in interlamellar d-spacing on incorporation of the reactants.

The X-ray diffraction data, plotted to show the region

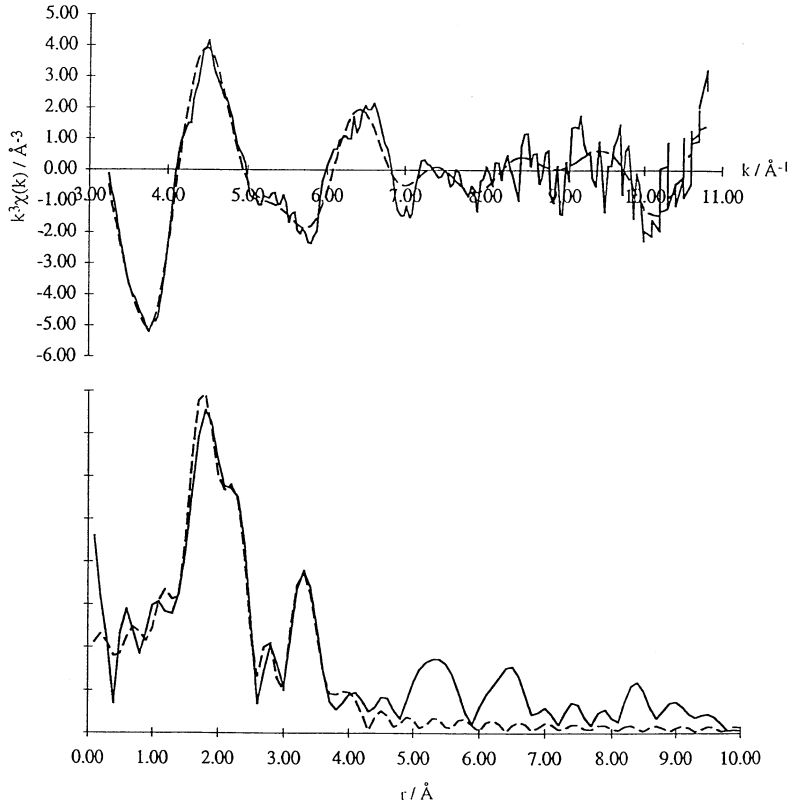

Fig. 4. Cu K-edge EXAFS spectrum, and its Fourier transform, for Zn(II)Al(III)-hydrotalcite/$CoPcTS^{4-}$, prior to catalysis. The theoretical fit is for six shells corresponding to nitrogen atoms at 1.94 Å (N = 2, $2\sigma^2 = 0.005$ Å^2), 2.14 Å (N = 2, $2\sigma^2 = 0.005$ Å^2) and 3.38 Å (N = 4, $2\sigma^2 = 0.005$ Å^2) and carbon neighbours 2.96 Å (N = 4, $2\sigma^2 = 0.044$ Å^2), 3.17 Å (N = 4, $2\sigma^2 = 0.08$ Å^2) and 3.62 Å (N = 4, $2\sigma^2 = 0.012$ Å^2): $F = 9.1\%$, $R = 33.69\%$.

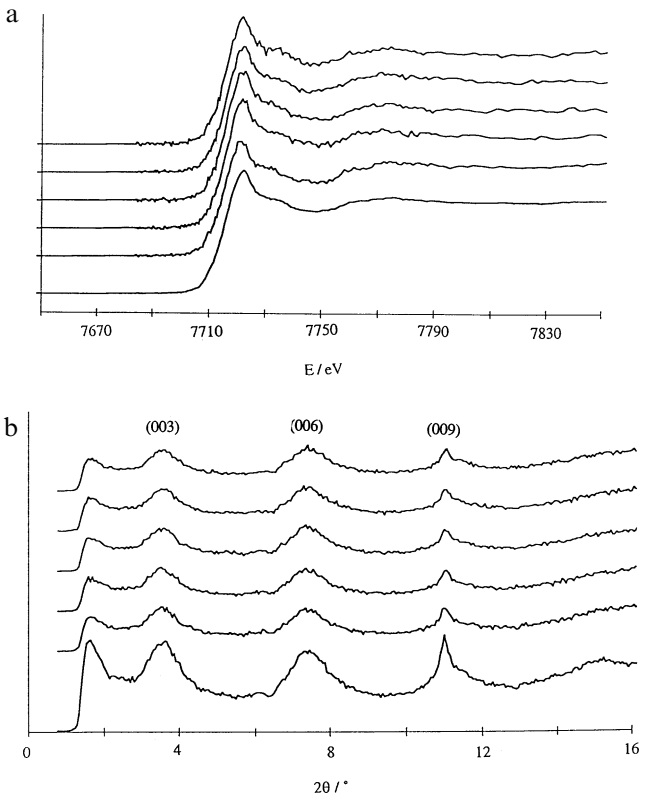

Fig. 5. (a) Co K-edge XANES plots and (b) stacked plot of the powder X-ray diffraction pattern recorded as the reactant mixture (as described in the text) was passed through a self-supporting wafer of Zn(II)Al(III)-hydrotalcite/$CoPcTS^{4-}$ catalyst at 30°C. In both diagrams, the bottom scan is for the catalyst prior to admission of liquid reactants. Time between subsequent scans is 10 min.

of the (003), (006) and (009) reflections (fig. 5b), show no changes over the time of the experiment, the *d*-spacing remaining at ca. 23 Å. This indicates that the layered hydrotalcite structure and the cobalt phthalocyaninetetrasulphonate anion are not destroyed during reaction. The drop in intensity between the first (bottom) scan and the subsequent scans is due to the admission of the reactant mixture to the cell. There is some evidence for variation in the XANES region during reaction (fig. 5b), though the changes are minor and appear around the first oscillation only. One reason for this may be that only those sites on the surfaces are accessible to reaction, and hence only those sites have undergone any changes.

The results demonstrate, however, the success of the new experimental reaction cell in enabling the recording of both EXAFS and XRD data simultaneously during solid/liquid heterogeneous catalytic reactions.

Acknowledgement

We gratefully acknowledge the support of EPSRC (rolling grant to JMT), Unilever (Postdoctoral research fellowship to IJS) and CCLRC for allocation of beamtime at Daresbury Laboratory.

References

[1] E. Dooryhee, G.N. Greaves, A.T. Steel, R.P. Townsend, S.W. Carr, J.M. Thomas and C.R.A. Catlow, Faraday Discussion Chem. Soc. 89 (1990) 119.
[2] E. Dooryhee, C.R.A. Catlow, J.W. Couves, P.J. Maddox, J.M. Thomas, G.N. Greaves, A.T. Steel and R.P. Townsend, J. Phys. Chem. 95 (1991) 4514.
[3] J.M. Thomas, C. Williams and T. Rayment, J. Chem. Soc. Faraday Trans. I 84 (1988) 2915;
T. Rayment, R. Schlögl, J.M. Thomas and G. Ertl, Nature 315 (1985) 311.
[4] P.J. Maddox, J. Stachurski and J.M. Thomas, Catal. Lett. 1 (1988) 191.
[5] I.J. Pickering, D. Madill, M. Sheehy, J. Stachurski, P.J. Maddox, J.W. Couves, E. Dooryhee and J.M. Thomas, J. Chem. Soc. Faraday Trans. 87 (1991) 3063.
[6] I.J. Pickering and J.M. Thomas, J. Chem. Soc. Faraday Trans. 87 (1991) 3067.
[7] J.W. Couves, J.M. Thomas, D. Waller, R.H. Jones, A.J. Dent, G.E. Derbyshire, B.R. Dobson, C.A. Ramsdale and G.N. Greaves, Nature 354 (1991) 465.
[8] J.M. Thomas and G.N. Greaves, Catal. Lett. 20 (1993) 337.
[9] B.S. Clausen, K. Grabaek, G. Steffensen, P.L. Hansen and H. Topsøe, Catal. Lett. 20 (1993) 23.
[10] J.M. Thomas and G.N. Greaves, Science 265 (1994) 1675.
[11] J.M. Thomas, G.N. Greaves and C.R.A. Catlow, Nucl. Instr. Meth. Phys. Res. B 97 (1995) 1.
[12] S.M. Clark, A. Nield, T. Rathbone, J. Flaherty, C.C. Tang, J.S.O. Evans, R.J. Francis and D. O'Hare, Nucl. Instr. Meth. Phys. Res. B 97 (1995) 98.
[13] J.S.O. Evans, R.J. Francis, D. O'Hare, S.J. Price, S.M. Clark, J. Flaherty, J. Gordon, A. Nield and C.C. Tang, Rev. Sci. Instrum. 66 (1995) 2442.
[14] F. Rey, G. Sankar, J.M. Thomas, P.A. Barrett, D.W. Lewis, C.R.A. Catlow, S.M. Clark and G.N. Greaves, Chem. Mater. 7 (1995) 1435.
[15] R.J. Francis, S.J. Price, J.S.O. Evans, S. O'Brien, D. O'Hare and S.M. Clark, Chem. Mater. 8 (1996) 2102.
[16] G. Sankar, J.M. Thomas, F. Rey and G.N. Greaves, J. Chem. Soc. Chem. Commun. (1995) 2549.
[17] G. Sankar and J.M. Thomas, in preparation.
[18] I.J. Shannon, F.Rey, G. Sankar, J.M. Thomas, T. Maschmeyer, A.E. Palomares, A. Corma, A.M. Waller, A.J. Dent and G.N. Greaves, J. Chem. Soc. Faraday Trans. 92 (1996) 4331.
[19] G. Sankar, F. Rey, J.M. Thomas, G.N. Greaves, A. Corma, B.R. Dobson and A.J. Dent, J. Chem. Soc. Chem. Commun. (1994) 2279.
[20] D. Bogg, M. Conyngham, J.M. Corker, A.J. Dent, J. Evans, R.C. Farrow, V.L. Kambhampati, A.F. Masters, D.N. McLeod, C.A. Ramsdale and G. Salvini, Chem. Commun. (1996) 647.
[21] J.M. Corker and J. Evans, J. Chem. Soc. Chem. Commun. (1994) 1027.
[22] T. Maschmeyer, R.D. Oldroyd, G. Sankar, J.M. Thomas, I.J. Shannon, J.A. Klepetko, A.F. Masters, J.K. Beattie and C.R.A. Catlow, Angew. Chem., submitted.
[23] B.S. Clausen, G. Steffensen, B. Fabius, J. Villadsen, R. Feidenhans'l and H. Topsøe, J. Catal. 132 (1991) 524.
[24] A. Skorobogathy and T.D. Smith, J. Mol. Catal. 16 (1982) 131.
[25] M.E. Pérez-Bernal, R. Ruano-Casero and T.J. Pinnavaia, Catal. Lett. 11 (1991) 55.
[26] G. Sankar, P.A. Wright, S. Natarajan, J.M. Thomas, G.N. Greaves, A.J. Dent, B.R. Dobson, C.A. Ramsdale and R.H. Jones, J. Phys. Chem. 97 (1993) 9550.
[27] N. Binsted, J.W. Campbell, S.J. Gurman and P.C. Stephenson, SERC Daresbury Laboratory Program (1991).